

1 ***Repression of YdaS Toxin is Mediated by Transcriptional Repressor***
2 ***RacR in the cryptic rac prophage of Escherichia coli-K12***

3 Revathy Krishnamurthi^{1,2}, Swagatha Ghosh², Supriya Khedkar^{1,2} and Aswin Sai Narain
4 Seshasayee²

5 1. Shanmuga Arts, Science, Technology & Research Academy, Thanjavur, Tamil Nadu,
6 India

7 2. National Centre for Biological Sciences, TIFR, Bangalore, India

8

9

10

11

12

13

14

15

16

17

18

19

20

21

22 **Abstract**

23 Horizontal gene transfer is a major driving force behind the genomic diversity seen in
24 prokaryotes. The *rac* prophage in *E.coli* K12 encodes a putative transcription factor RacR,
25 whose deletion is lethal. We have shown that the essentiality of *racR* in *E.coli* K12 is
26 attributed to its role in transcriptionally repressing a toxin gene called *ydaS*, which is
27 coded adjacent and divergently to *racR*.

28 **Introduction**

29 Horizontal Gene Transfer (HGT) contributes to the vast genome diversity seen in
30 prokaryotes. The size of the genomes of *E.coli* varies from 3.97 Mb to 5.85 Mb. The core
31 genome constitutes only ~10% of the gene families represented across these *E.coli*
32 genomes. The rest of the genetic content is variable across strains and often found in
33 genomic islands [1]. Many virulence factors and determinants of antibiotic resistance are
34 known to be horizontally acquired, and encoded for example in autonomously replicating
35 plasmids and chromosomally replicating prophages [2] [3].

36 The genome of the laboratory strain *E.coli*-K12 comprises nine cryptic prophages which
37 constitute 3.6% of its total genome. The successful maintenance of any horizontally
38 acquired element depends on the conventional selection advantage that it provides to the
39 host and as well as addiction imposed on the host by selfish genetic modules.

40 Conventional selection is defined by the benefit it provides the host under the given
41 condition. A horizontally acquired gene may integrate into the rest of the cellular network
42 by affecting the function of genes belonging to the core genome, or that of unrelated
43 horizontally acquired elements[4][5]. For example, a phenotypic microarray study has
44 shown that the nine cryptic prophages in *E.coli*-K12 help the bacterium survive under
45 various stresses [6].

46 Several horizontally acquired elements also carry addiction molecules, including

47 Restriction Modification (R-M) and Toxin Antitoxin (T-A) systems [7][8]. Loss of such
48 modules can result in post-segregational killing, which encourages the maintenance of
49 such DNA [9]. Some T-A systems and R-M systems may have eventually evolved functions
50 which provide benefit to the host, including roles in programmed cell death [10][11].

51 During an effort towards addressing the regulatory roles of horizontally acquired
52 transcriptional regulators, we learnt that the poorly characterized gene *racR* which is a
53 putative repressor of the *rac* prophage is an essential gene in *E.coli* K12. Using a
54 combination of genetics, biochemistry and bioinformatics, we present evidence that RacR
55 is indeed a transcriptional repressor. We have shown that RacR binds to its own regulatory
56 region. The adjacent and divergently coded *ydaS* and *ydaT* together encode a toxin whose
57 expression is repressed by the function of RacR. Thus *ydaST* – *racR* module forms a
58 toxin-repressor combination, which makes this RacR regulator essential to the cell.

59 **Results**

60 **RacR is an essential transcriptional regulator**

61 The *rac* prophage is a cryptic prophage found in *E.coli*. It is a mosaic prophage. It is 23 kb
62 long, and encodes 29 genes in *E.coli* K12. However, its size and gene content vary across
63 *E.coli* strains, with only a few highly conserved genes, which include *recE* – involved in
64 alternative homologous recombination pathway, and *trkG*, a potassium ion permease
65 [Figure 1A].

66 Among the less conserved portion of the *rac* prophage is a predicted transcription factor
67 called RacR. It contains a weak helix-turn-helix motif and at best is very distantly related to
68 the lambda *cI* repressor (15% identity by Needleman-Wunsch global alignment). Its
69 deletion is presumed to be lethal. The Keio collection of *E.coli* single gene deletion
70 mutants does not contain $\Delta racR$ [12], and we were unable to delete *racR* by homologous
71 recombination. Nevertheless, the entire *rac* prophage could be deleted (we refer to this as

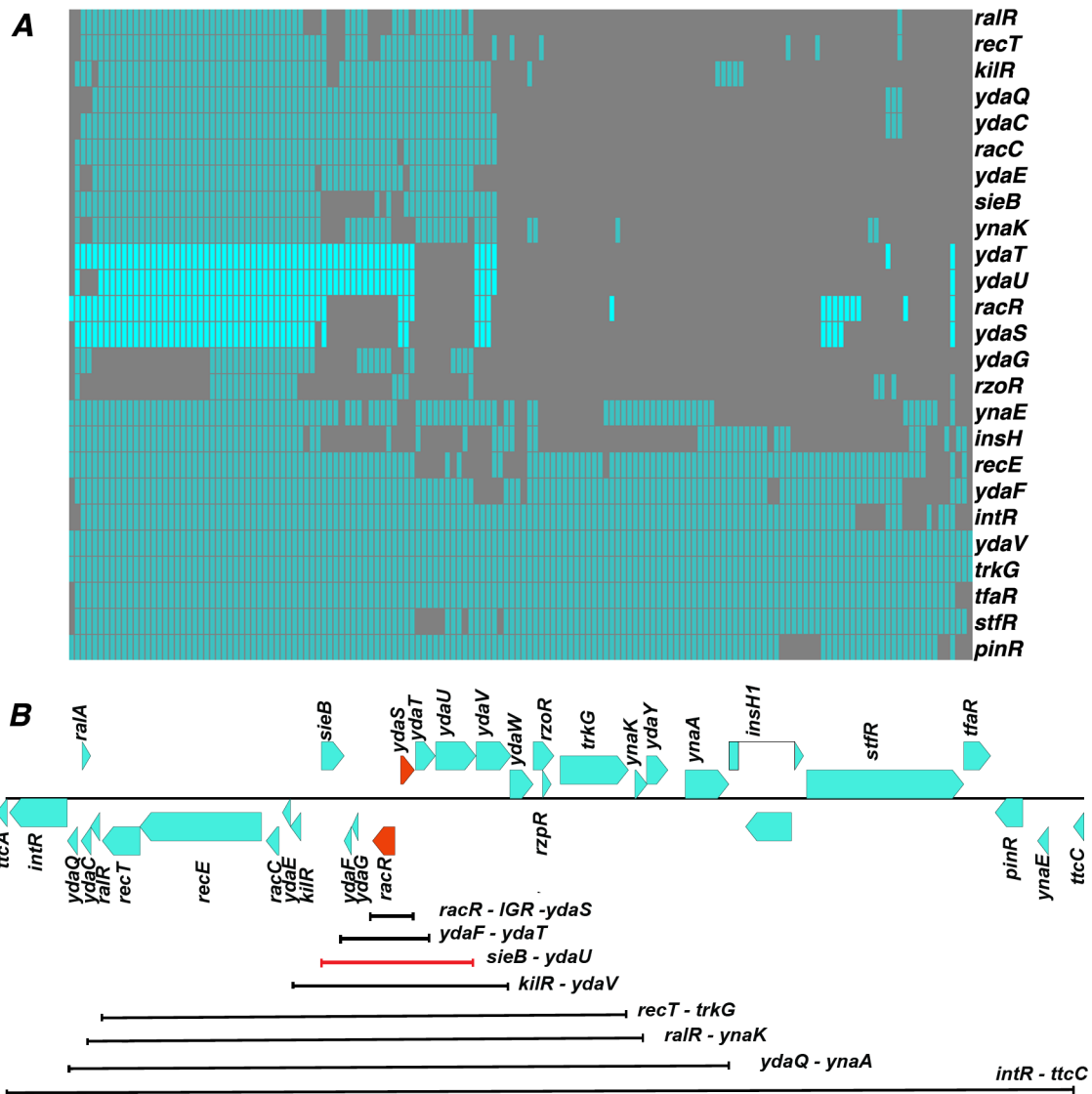


Figure1: A) Matrix showing the conservation of *rac* prophage genes across 154 *E.coli* genomes. Absence of any gene is indicated by grey and the presence by cyan. The genes *racR*, *ydaS*, *ydaT* and *ydaU* are shown in bright cyan. Note that the presence of *ydaS* is always accompanied by the presence of *racR*. B) Map of *rac* prophage showing the putative regulatory genes in orange. The lines indicates the eight *racR* inclusive regions deleted. The line marked in red shows the region deleted from *sieB* -*ydaU* which left the gene *kilR* in the absence of *racR*.

72 Δrac here), and the prophage excises at high rates in certain genetic backgrounds [13].
 73 Hence we hypothesized that RacR could be a repressor of a toxin in the same prophage.
 74 Because the *rac* prophage carries a previously reported toxin called KilR - an inhibitor of
 75 cell division [14] - we initiated our screen for the toxin by attempting to delete *racR* in the
 76 $\Delta kilR$ strain. However, we found that $\Delta racR$ could not be obtained even in a $\Delta kilR$
 77 background.

78 We then deleted successively shorter *racR*-inclusive segments of the prophage. If a
79 deletion attempt removed *racR* but not the toxin that RacR might repress, we would not
80 recover the mutant. The smallest deletion we obtained by this approach included *racR*, its
81 neighboring, divergent gene *ydaS* and the common intergenic region (henceforth referred
82 to as IGR) between them [Figure 1B]. Thus the absence of *ydaS* and the common IGR
83 between *racR* and *ydaS* is a suppressor of the lethality of $\Delta racR$.

84 Despite several attempts, we were unable to delete *racR* in $\Delta ydaS$ without disturbing the
85 IGR between them. However, we obtained $\Delta racR$ with its IGR intact in a $\Delta ydaS-T$
86 background. *ydaT* is encoded in tandem and downstream of *ydaS* and might be part of the
87 same operon.

88 **Over expression of *ydaS* and *ydaS-T* reduces growth**

89 We tested the toxicity of *ydaS*, *ydaT* and *ydaS-T* by cloning these genes under the
90 *araBAD* promoter in pBAD18. Expression of these cloned genes was induced in both
91 wildtype and Δrac with 0.1% L-arabinose. We found that the expression of *ydaS* and
92 *ydaS-T* causes rapid growth inhibition after induction in both wildtype and Δrac
93 [Supplementary Figure S1]. We collected samples at 5 hours and 14 hours after induction
94 and spotted these on agar plates. Cells expressing *ydaS* and *ydaS-T* from pBAD18 did not
95 grow on these plates [Figure 2A]. The expression of *ydaT* alone did not have any inhibitory
96 or lethal effect on the wild type or the Δrac prophage strain.

97 Further, we quantified the live and dead cell populations after the induction of *ydaS*, *ydaT*
98 and *ydaS-T* by FACS using Propidium Iodide (PI) as the marker for dead cells. Results
99 from six independent trials show that *ydaS* and *ydaS-T* expression, irrespective of the
100 strain background, leads to loss of cell viability [Figure 2B]. We noticed that *ydaS-T*
101 expressing cells were lengthier than the *ydaS* or *ydaT* expressing cells [Supplementary
102 Figure S2].

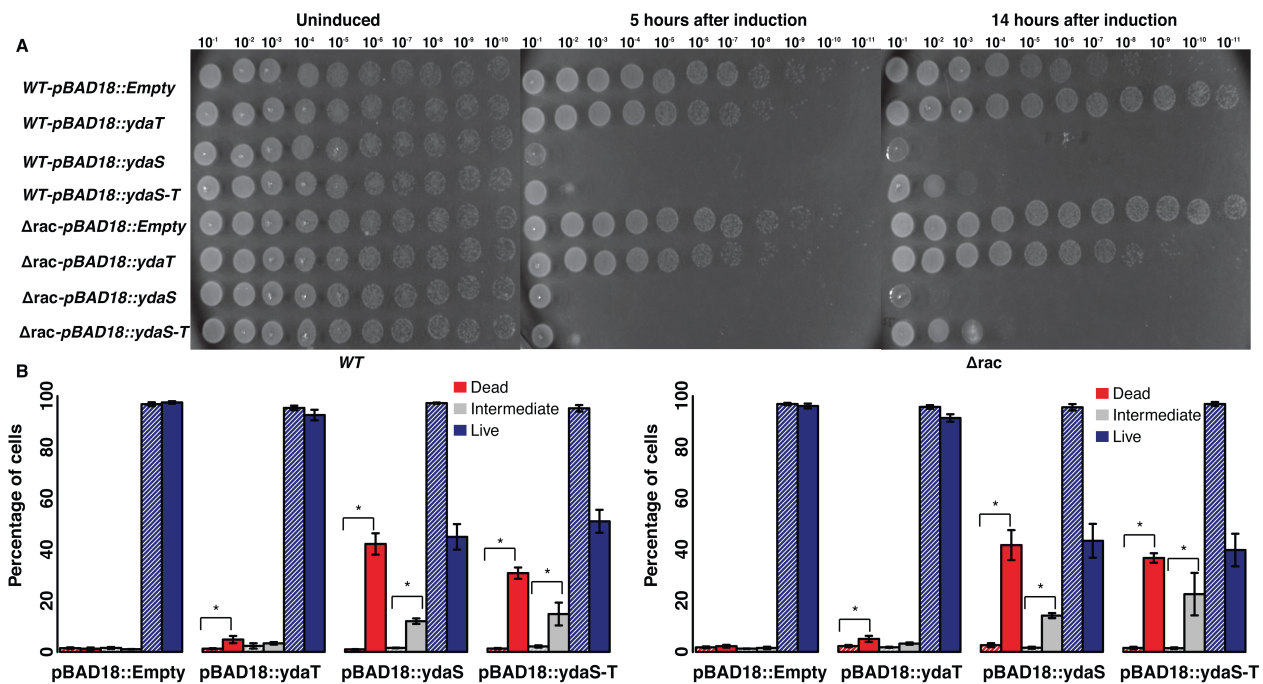


Figure 2 : A) Log and stationary phase cultures of *pBAD18-ydaS*, *pBAD18-ydaT*, *pBAD18-ydaS-T*, and Empty vector in wild type and in Δrac background, grown in the presence or absence of 0.2% L-Arabinose, were spotted on the LB plate without arabinose. B) Live Dead Assay of *pBAD18-ydaS*, *pBAD18-ydaT*, *pBAD18-ydaS-T* and Empty vector in wild type and in Δrac backgrounds. The cells were collected after 5 hours of induction and treated with Propidium Iodide (PI) to mark the dead cells. Bar graph represents the percentage of dead, intermediate and live population of cells in uninduced (striped) and induced (filled) cultures. * corresponds to p -value < 0.01; Wilcoxon rank sum test between induced and uninduced constructs. Error bar here represents the standard error computed from six independent trials (Three biological and two technical replicates).

103 Together, these results show that the expression of *ydaS* and *ydaS-T* is lethal, and *ydaS*
 104 and *ydaT* do not form a TA pair as predicted earlier [15]. *YdaS* is critical to cell killing, and
 105 *YdaT* may enhance the lethal effect of *YdaS* while not being toxic on its own.

106 Co occurrence of *racR* and *ydaS* implies interaction between them

107 Functionally related genes tend to be conserved together across genomes [16]. We
 108 examined the conservation of genes of the *rac* prophage across 154 *E.coli* genomes. Bi-
 109 directional best hit search for orthologs confirmed the mosaic nature of the *rac* prophage.
 110 In fact, more than 50% of the strains have lost half of the prophage. The genes that are
 111 well conserved across the genomes are those, such as *recE* and *trkG*, which have
 112 documented functions in the host. Some classical phage genes like *intR*, *pinR*, *stfR*, *tfaR*,
 113 *ydaF* and *ydaV* are conserved in more than 85% of the strains analyzed.

114 We observe that the known toxin genes in the prophage are lost in most of the strains and
115 where present, are always accompanied by its cognate antitoxin genes. RalR-RalA is a
116 known type I T-A system in the same prophage^[17]. We observe that the RalR toxin is
117 conserved only in 36.3% of the strains we analyzed; the corresponding non-coding anti-
118 toxin gene was found in all these strains. KilR, previously reported as a FtsZ inhibitor, was
119 found in 48% of the strains in this analysis; its antitoxin, if any, is unknown.

120 YdaS is present only in 33.7% of the strains analyzed and we observe that it always co-
121 occurs with RacR [Figure 1A]. A few strains encoded *ydaT* gene in the absence of *racR*;
122 however the IGR was lost in these strains, and certain point mutations were found in the
123 *ydaT* gene. We also observe that YdaT expression on its own, in the absence of YdaS, is
124 not lethal. Thus, genome context analysis suggests a functional interaction between RacR
125 and YdaS(-T).

126 **Expression of *ydaS* is kept silent under normal physiological conditions**

127 In order to examine the expression of RacR and YdaS in vivo, we tagged these two genes
128 with C-terminal 3X-FLAG (DYKDDDDK). Western blotting using an anti-FLAG antibody
129 showed that RacR was expressed in all the phases of growth. However, YdaS expression
130 could not be detected in our experimental conditions [Fig 3A]. An absolute protein
131 quantification study reported by Li *et.al* 2014., also shows low copy number for YdaS ^[18].

132 Analysis of various publicly available and in-house RNA-seq data showed that the
133 expression of *ydaS* is comparable to that of *bg/G*, a well-characterized transcriptionally
134 silent cryptic gene ^[19]. *racR* was among the most highly expressed genes in the *rac*
135 prophage, but only to a level comparable to that of the lac repressor gene [Supplementary
136 Figure S3]. These show that YdaS is not expressed in *E.coli*, and, in light of the genetic
137 experiments reported above, lead to the hypothesis that RacR is a repressor of this toxin.

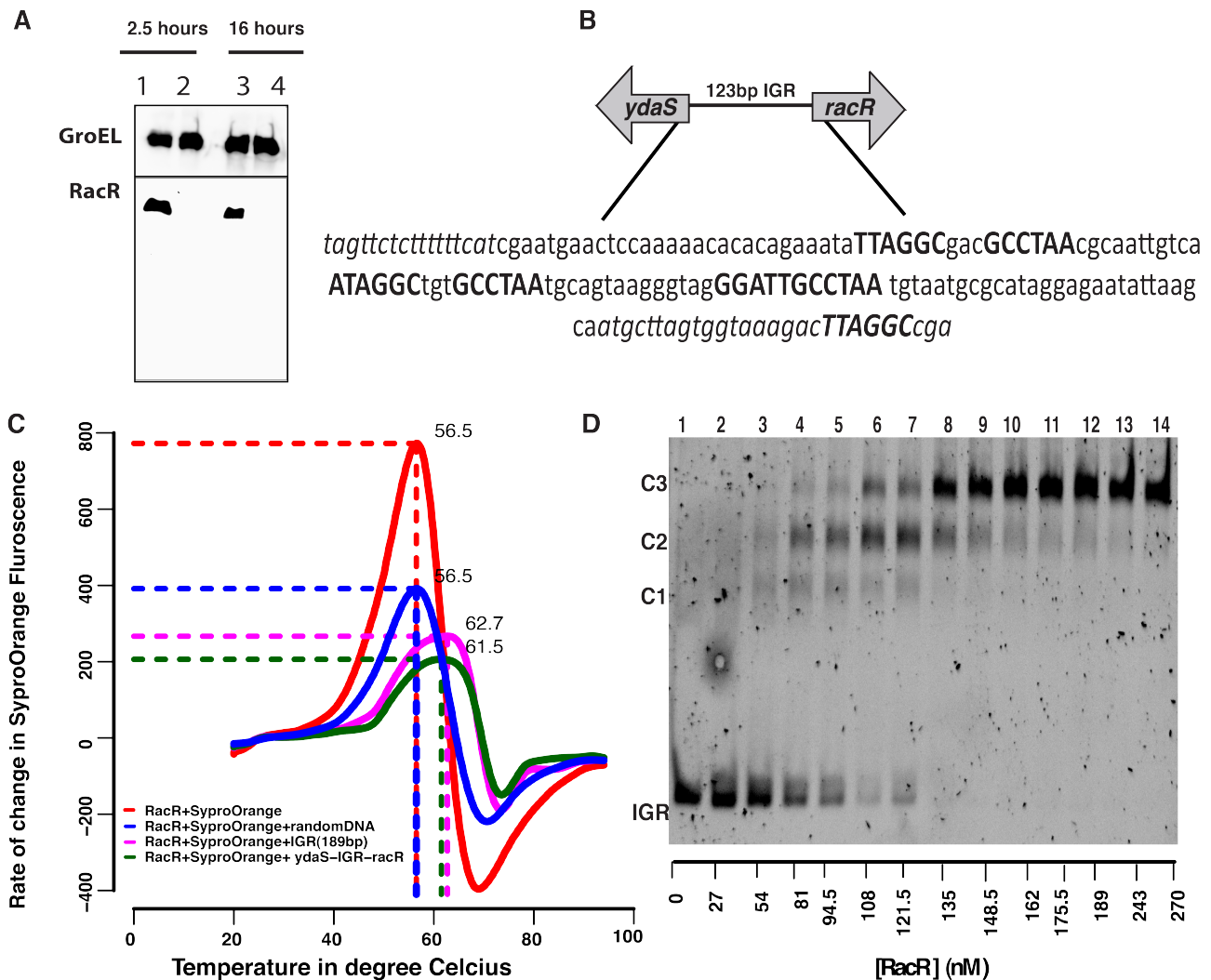


Figure 3: A) Western blot showing the expression of RacR; YdaS expression could not be detected. The top panel showing GroEL as loading control and the bottom panel showing the RacR expression during log and stationary phase. 20 µg of total protein was used. B) Intergenic Region (IGR) between *ydaS* and *racR* showing the repeat elements with slightly varying sequence in three different regions (bold sequence). Note that the *ydaS* and *racR* are coded divergently and in opposite strands. C) Thermal Shift Assay showing ~5°C shift in the TD of RacR in the presence of IGR. D) Non-radioactive Electrophoretic Mobility Shift Assay showing the binding of RacR with IGR with distinct complexes marked as C1, C2 and C3. 15 nM of 123bp IGR was titrated against increasing concentration of RacR from 27 nM to 270 nM (Lane 2-14). Lane 1 shows only 15nM of IGR without RacR.

139 Binding of RacR in the IGR

140 RacR comprises a Helix Turn Helix (HTH) motif, and hence we investigated if it binds to
 141 DNA. The 123 bp IGR between *racR* and *ydaS* contains three slightly variant repeats of
 142 “GCCTAA” and its inverse “TTAGGC” [Figure 3B]. This is similar to the regulatory region of
 143 lambda phage, which is bound by C1 and Cro, even though the exact sequences bound by
 144 the proteins are different.

145 To test for the binding of RacR to the IGR, we first performed a thermal shift assay with
146 purified RacR and various nucleic acid sequences. The thermal shift assay measures the
147 thermal denaturation temperature of a test protein. A change in this temperature in the
148 presence of a ligand might argue in favour of an interaction between the protein and the
149 ligand. We found that the T_D of RacR increased by $\sim 5^\circ\text{C}$ in the presence of *racR*-IGR-
150 *ydaS* or in that of a 189 bp sequence upstream of *ydaS* and including the IGR [Figure 3C].
151 The extended 189 bp region, including a portion of the *racR* gene, was chosen for this
152 experiment because this included an additional half-site of the above-mentioned
153 palindrome.

154 We then performed a chromatin IP of RacR::3xFLAG to test for the binding of RacR to the
155 IGR *in vivo*. By performing qPCR against the DNA thus recovered, we found that the IGR
156 was 2.5 fold enriched in comparison to a random region [Supplementary Figure S4-A].
157 Finally, we performed Electrophoretic Mobility Shift Assay (EMSA) to investigate the
158 binding of purified RacR to the IGR. RacR formed three distinct complexes in the presence
159 of the IGR [Figure 3D]. EMSA with a 49-bp DNA upstream of *ydaS*, containing a single
160 copy of the repeat, also showed binding to RacR [Supplementary Figure S4-B]. Consistent
161 with the view that the three palindromic repeats might be the sites to which RacR binds,
162 we found only a single protein DNA complex with the 49-bp segment of the IGR. Thus, we
163 show binding of RacR to the intergenic region between *racR* and *ydaS* both *in vitro* and *in*
164 *vivo*.

165 **Transcriptional repression of *ydaS* is mediated by RacR binding to the IGR**

166 Finally, to test whether the binding of RacR represses *ydaS*, we cloned the IGR upstream
167 of *gfp-mut2* in pUA66. We monitored the promoter activity of pUA66::IGR-*gfp-mut2* in
168 $\Delta ydaS$ -*T* and in $\Delta racR$ - $\Delta ydaS$ -*T* for 25 hours. We observed that the *ydaS* promoter is
169 active only in $\Delta racR$ - $\Delta ydaS$ -*T*; no fluorescence from *gfp-mut2* could be detected in $\Delta ydaS$ -
170 *T* [Figure 4A].

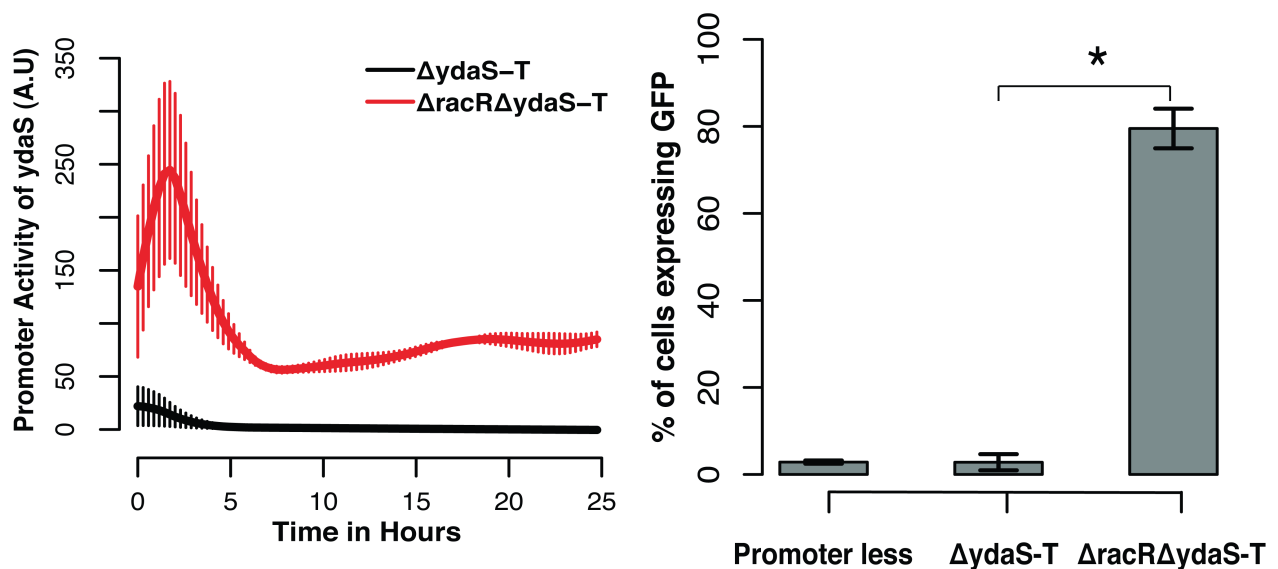


Figure 4: A) IGR cloned in the low copy pUA66 plasmid, showing promoter activity of *ydaS* in $\Delta ydaS-T$ (black line) and in $\Delta racR\Delta ydaS-T$ (red line) strains. B) Bar graph representing the percentage of cells showing *ydaS* promoter Activity. * corresponds to p -value < 0.01; t -test. Error bar here represents the standard deviation computed from three independent trials.

171 The maximal *ydaS* promoter activity was observed in the log phase ($OD_{600} \sim 0.2-0.3$). We
172 tested the expression of *gfp-mut2* from these strains grown to mid-exponential phase
173 using FACS. The distribution of fluorescence from pUA66::IGR-*gfp-mut2* in $\Delta ydaS-T$ was
174 similar to that of the promoterless control where most cells were GFP negative. In contrast,
175 in $\Delta racR\Delta ydaS-T$, nearly 80% of the cells were GFP positive [Figure 4b]. Thus single-
176 copy availability of RacR from the chromosome appears to be sufficient to suppress the
177 activity of the *ydaS* promoter from a multicopy ($N = 3-4$) plasmid. Thus, RacR represses
178 transcription of *ydaS*.

179 Discussion

180 We have shown that the expression of *ydaS* and *ydaS-T* is lethal, and we attribute the
181 essentiality of *racR* to its role in repressing the expression of this toxin. Earlier studies
182 have shown the presence of two toxins - KilR and RaIR - in the *rac* prophage [14][17]. In the
183 present work, we suggest that that YdaS-T is yet another toxin encoded by the *rac*
184 prophage. We do not know how this toxin effects cell killing, and whether other genes in
185 the operon to which *ydaS* and *ydaT* belong contribute to cell killing.

186 RacR is a repressor of *ydaS-T*, and this module is an example of a toxin-repressor system.
187 In general, essential transcription factors are rare in *E.coli*. The essentiality of RacR is
188 purely by virtue of its role in keeping a toxin transcriptionally silent. RacR is unlikely to
189 have too many additional targets, because its expression level - based on RNA-seq - is
190 very similar to that of the highly specific Lac repressor.

191 Among the few essential transcription factors in *E.coli* is the anti-toxin MazE. *mazE* and
192 *mazF* are encoded on the same operon, unlike *racR-ydaS*, which make a divergent gene
193 pair. The anti-toxin activity of MazE is primarily by protein-protein interactions with the toxin
194 MazF. In fact, the binding of MazE to the DNA is enhanced when in complex with MazF^[20].
195 Yet another essential transcription factor is the antitoxin MqsA, which again sequesters its
196 cognate toxin MqsR. Unlike the conditional cooperativity displayed by MazE and MazF in
197 binding to the DNA, the high stability of the MqsR-A complex makes the protein-protein
198 interaction mutually exclusive of MqsA-DNA interactions^[21]. In both these cases, it is
199 apparent that the activity of the transcriptional repressor does not entirely prevent the
200 expression of the toxin. In our case however, we could not detect the presence of YdaS
201 protein, the expression level of the *ydaS* transcript is comparable to that of a bonafide
202 cryptic gene across tens of RNA-seq datasets, and in the presence of RacR we cannot
203 detect any activity from the *ydaS* promoter fused to *gfp-mut2*. The expression of YdaS-T is
204 toxic, independent of the presence of RacR (wildtype vs. Δrac), which argues against the
205 possibility of RacR interacting physically with YdaS / YdaT in suppressing its activity.

206 It is arguable whether RacR-YdaST can be called a toxin-antitoxin system, because the
207 fact that the activity of the toxin is totally suppressed at the level of transcription initiation
208 itself might render post-segregational killing downstream of the loss of the module
209 impossible.

210 We propose that RacR could be functionally similar to the CI repressor of lambda
211 prophage. The *rac* prophage has lost many of its structural genes when compared to the

212 lambda phage [Supplementary Fig S5]. However, the organization of regulatory elements
213 in the *rac* prophage [Figure 3B] is similar to the *ci*-Cro switch of lambda prophage [22].
214 There are three repeat elements in the IGR, which might be the operator of this prophage.
215 Our observation on the formation of three distinct DNA-Protein complexes of the 123 bp
216 IGR with increasing concentrations of RacR, suggests that the IGR might act as a complex
217 regulatory switch that resembles the regulatory region of *ci*-cro of lambdoid phages [23].

218 **Materials and Methods**

219 **Media, Strains and Plasmid Construction**

220 *E.coli* K12 MG1655 from CGSC was used and grown at 37°C in Luria Broth (LB) or LB
221 Agar (HiMedia). The antibiotic resistant strains were grown in antibiotics wherever
222 required; ampicillin (100 µg/mL), kanamycin (50 µg/mL) or chloramphenicol (30 µg/mL)
223 were used. All the knock out strains were constructed by using the one step inactivation
224 method as described by Datsenko *et al.* using pKD13 as the template plasmid for the
225 kanamycin resistance cassette amplification [24]. Tagging of *racR* with 3xFLAG at the C
226 terminal end was done using the pSUB11 plasmid [25]. Ectopic expression of *racR*, *ydaS*,
227 *ydaT* and *ydaST* were achieved by cloning them between EcoRI and Sall site of pBAD18;
228 this brings the genes under the arabinose inducible *araBAD* promoter. The plasmid for the
229 promoter activity was constructed by cloning the IGR in the low copy vector pUA66
230 between XhoI and BamHI sites. The list of strains and plasmids used in the current study
231 is given in Supplementary Table1 and the primers used for gene deletion, validation and
232 cloning are listed in Supplementary Table 2.

233 **Growth Curve and Spotting Assay**

234 Growth curve was monitored in a 96 well plate with the final volume of 200µl using Tecan
235 F200 reader. Overnight culture was inoculated in the ratio of 1:100 and allowed to grow till
236 0.4 OD. This was further diluted in fresh medium to 0.01 OD with or without 0.1% L-
237 arabinose and A_{600} was recorded for 14 hours. For the spotting assay, appropriate
238 overnight cultures were inoculated in LB broth containing 100 µg/mL ampicillin at 1:100
239 dilution, with or without 0.2% L-arabinose. The cells were collected after 5 hours and 14
240 hours of inoculation, serially diluted and spotted on LB agar plates containing ampicillin
241 without arabinose.

242

243 **FACS**

244 Overnight culture of the respective strains were inoculated in LB broth at 1:100 dilution
245 with or without 0.2% L-arabinose. Samples were collected after 5 hours of induction,
246 pelleted down, washed and resuspended in 500 μ l of saline (0.9% sodium chloride w/v).
247 Exponentially growing cells were used as live-cell control and cells subjected to 80°C for
248 10 minutes were used as dead-cell control. Propidium Iodide (PI) solution (5 μ l of 1 mg/ml)
249 was added to all the vials 10 minutes before acquisition of data in BD FACS Calibur.
250 Around 20,000 cells were acquired for each sample using 488 nm excitation laser and the
251 emission was recorded from FL2 channel that uses 585/42 BP filter, to collect the PI
252 intensity. Intermediate population in this study is described as cells that fall between the
253 region of live unstained control and dead control.

254 Exponential culture of $\Delta ydaS-T$ and $\Delta racR-\Delta ydaS-T$ containing pUA66::I $GR-gfp-mut2$
255 were pelleted, washed and resuspended in saline. GFP intensity was monitored using FL1
256 channel that uses 530/30 BP filter. Strain containing empty pUA66::*gfp-mut2* was used to
257 set the background fluorescence and GFP intensity above this background was marked as
258 positive. Data was analyzed using Flowing software (www.flowingsoftware.com/).

259 **Bi-Directional Search for orthologous genes**

260 Genomes of 154 completely sequenced *E.coli* strains were downloaded from NCBI refseq
261 ftp site. A bi-directional search for orthologous genes of the *rac* prophage, excluding
262 pseudogenes, was performed using phmmer (Version 3.1). The E-value threshold used
263 was 10^{-20} . An ortholog presence-absence matrix was hierarchically clustered based on
264 Euclidean distance with centroid linkage. Clustering was done using Cluster3
265 (bonsai.hgc.jp/~mdehoon/software/cluster/) and the heat map was generated using
266 matrix2png (<http://www.chibi.ubc.ca/matrix2png/>) .

267

268 **RNA - Seq Data Analysis**

269 Raw reads from 15 different RNA-seq studies (with total of 61 fastq files) were obtained
270 either in-house or from the NCBI GEO, or the EBI Array Express databases
271 [Supplementary Table 3]. The SRA files from GEO were converted to fastq using fastq
272 dump. Reads from the fastq file were aligned to NC_000913.3 genome using bwa. The
273 aligned files were sorted using sam tools. Further, these sam files were used to get read
274 counts per nucleotide, from which read counts per gene was generated. RPKM (Reads per
275 Kilobase of transcript per Million mapped reads) was calculated by normalizing the raw
276 read counts to the length of the gene and further by the total number of mapped reads for
277 each fastq file. The distribution of RPKM values of the *rac* prophage genes were plotted as
278 a boxplot, along with those of the *bgl* operon genes and *lacI* as reference. Because
279 differential expression was not a goal of this study, more state-of-the-art normalization
280 methods such as those used by EdgeR or DEseq were not required.

281 **Western Blotting**

282 Total protein of *E.coli*-K12 cells was prepared and quantified using BCA Assay and 20 μ g of
283 total protein was loaded in 15% SDS polyacrylamide gel. The gel was subjected to
284 electrophoresis at 120V for 1 hour and proteins were transferred to a nitrocellulose
285 membrane. Monoclonal anti-FLAG antibody (Sigma) was used to bind the specific protein
286 to which the FLAG is tagged, and the signal was detected using (HRP) Horse Radish
287 Peroxidase conjugated anti-mouse IgG. HRP luminescence was further detected by West
288 Dura reagent (Thermo scientific). Digital images of the blots were obtained using an LAS-
289 3000 Fuji Imager.

290 **Chromatin Immuno Precipitation**

291 Immuno precipitation was done as described by Kahramanoglou et al. [26] except that cell
292 lysis and DNA shearing were coupled together using Bioruptor (Diagenode) with 35 cycles

293 (30 seconds ON and 30 seconds OFF) at high setting. Immuno precipitated samples were
294 quantified with specific primers for the 123 bp intergenic region (IGR) and a random primer
295 (*wza*), which is not the part of the *rac* prophage, using quantitative PCR. The fold
296 enrichment was calculated using $2^{-(\Delta\Delta Ct)}$ as described by Mukhopadhyay et al.[27].

297 **RacR purification**

298 RacR was cloned between the NdeI and XhoI restriction sites in a pET28a expression
299 vector with the C-Terminal His tag. After confirmation of its sequence and orientation, this
300 plasmid was transformed in the expression strain C41(DE3). A single colony of the C41
301 strain containing the pET28a::*racR* plasmid was inoculated in 5 mL LB containing 100
302 $\mu\text{g/mL}$ ampicillin. This overnight culture was diluted to 1:100 ratio in 10 mL of fresh LB for
303 raising the secondary inoculum. When the secondary culture reached 0.4 OD, it was
304 seeded in fresh 1L LB in a 3L baffled flask at 37°C. When the culture reached 0.6 OD,
305 RacR expression was induced by adding IPTG at the final concentration of 100 μM and
306 the flask was incubated at 25°C for 5 hours. The culture was harvested and the cells were
307 resuspended in 100 mL of Lysis buffer (50 mM Tris-pH 8.5, 500 mM NaCl, 5% Glycerol, 1%
308 NP-40, 1x Sigma Protease Inhibitor Cocktail). The resuspended cells were sonicated for
309 30 cycles (30 seconds ON and 30 seconds OFF). Further, the lysate was passed through
310 equilibrated 1 mL pre-packed Histrap column (Invitrogen) at a flow rate of 0.5mL/minute.
311 Then the column was washed with 50 mL of elution buffer (50 mM Tris- pH 8.5, 500 mM
312 NaCl, 5% Glycerol) containing 10 mM imidazole, and then with 20 mL of elution buffer
313 containing 50 mM imidazole and 100 mM imidazole respectively. Finally, RacR was eluted
314 with 10 mL of elution buffer containing 250 mM imidazole. Purified RacR was further
315 passed through a Superdex 200 10/300 size exclusion column, which was pre equilibrated
316 with the same elution buffer without imidazole.

317 **Thermal Shift Assay**

318 0.3 μM of DNA (*ydaS* with 189 bp upstream of it including a portion of *racR*, *racR*-IGR-

319 *ydaS* or random DNA) was mixed with 3 μ M of purified RacR in the presence of 20x
320 Sypro® Orange (Sigma Aldrich), and the final volume of the reaction was adjusted to 20
321 μ L with RacR elution buffer. Three replicates of each sample were loaded in a 384 well
322 plate and sealed with optical adhesive cover. The fluorescence spectrum in 635 nm - 640
323 nm bin was recorded using ABI Via7 PCR with the standard melt curve experiment setting
324 in which the temperature ranged from 20°C to 95°C at the rate of 1°C per minute.
325 Denaturation temperature (T_D) was reported as the temperature at which the maximum
326 dF/dT was recorded, where dF/dT is the rate of change in Sypro® Orange fluorescence
327 with respect to the temperature. The data was processed and plotted using a custom R
328 script to calculate dF/dT .

329 **Electrophoretic Mobility Shift Assay**

330 The entire 123 bp IGR was PCR amplified and gel purified. Polyacrylamide gel of 6% was
331 prepared from 40% acrylamide:bisacrylamide (80:1) stock and allowed to polymerize for 2
332 hours. The gel was pre-run for 30 minutes at 70 V and the wells were washed before
333 sample loading. 20 nM of DNA was mixed with increasing concentration of RacR in 10x
334 binding buffer (100 mM Tris Buffer-pH 8, 10 mM EDTA, 1M NaCl, 1mM DTT, 50% Glycerol,
335 0.1 mg/mL BSA) with 20 μ L final volume in 0.2mL PCR tubes. These tubes were incubated
336 at room temperature for 1 hour. After incubation, samples were mixed with 2.2 μ L of 10x
337 loading dye (10 mM Tris-pH 8, 1 mM EDTA, 50% glycerol, 0.001% bromophenol blue,
338 0.001% xylene cyanol.) and run at 70 V in room temperature for 90 minutes. The gel was
339 stained using SyBr® Green (Thermo Scientific) for 15 minutes. The stained gel was
340 washed in distilled water twice and imaged using a Lab India Geldoc system.

341 **Promoter Activity**

342 Promoter activity of the *ydaS* IGR was monitored by transforming the pUA66::*IGR-gfp-*
343 *mut2* construct in $\Delta ydaS-T$ and in $\Delta racR-\Delta ydaS-T$. M9 Media with 0.2% glucose was used
344 to culture the strains. Overnight culture containing the plasmid in the respective

345 background strain was inoculated in the ratio of 1:100 in a 96 well flat transparent black
346 plate (corning) with total volume of 200 μ L . The optical density (OD 600 nm) and the GFP
347 intensity (excitation at 485 nm and emission at 510 nm) were measured using the Tecan
348 multimode reader at every 16 minutes interval with continuous shaking in between at
349 37°C. The background optical density is subtracted by using the optical density obtained
350 from the blank well. The background fluorescence intensity was subtracted by using the
351 intensity obtained from the strain that has promoterless empty vector. Promoter Activity
352 was calculated as rate of change in the GFP intensity normalized by the average OD for
353 the given time point. $PA = (\text{smoothed}) \, dGFP/dt / (\text{smoothed})(OD1+OD2/2)$ [28]. Data
354 processing and analysis were done using custom R script.

355 **Acknowledgements**

356 R.K is supported by DST INSPIRE fellowship (DST/INSPIRE Fellowship/2010). S.G and
357 S.R is supported by DBT grant (BT/PR5801/INF/22/156/2012). S.K is supported by CSIR
358 fellowship (09/860(0122)/2011-EMR-I). A.S.N.S is funded by Ramanujan fellowship
359 (DST:SR/S2/RJN-49/2010). The authors thank the PTC of CCAMP and NCBS CIFF for
360 technical support. We thank Aalap Mogre for providing his RNA seq analysis pipeline and
361 Parul Singh for providing transcriptome data. We thank Dr. Ramaswamy and Dr.
362 Shivaprasad for granting accession to use their lab instruments.

363

364

365

366

367

368

369 **Bibliography**

- 370 1. Lukjancenko, O., Wassenaar, T. M. & Ussery, D. W. Comparison of 61 Sequenced
371 *Escherichia coli* Genomes. *Microb. Ecol.* 60, 708–720 (2010).
- 372 2. Thomas, C. M. & Nielsen, K. M. Mechanisms of, and barriers to, horizontal gene
373 transfer between bacteria. *Nat. Rev. Microbiol.* 3, 711–721 (2005).
- 374 3. Zhang, X. et al. Quinolone Antibiotics Induce Shiga Toxin–Encoding Bacteriophages,
375 Toxin Production, and Death in Mice. *J. Infect. Dis.* 181, 664–670 (2000).
- 376 4. Atlung, T. & Brøndsted, L. Role of the transcriptional activator AppY in regulation of the
377 *cyx appA* operon of *Escherichia coli* by anaerobiosis, phosphate starvation, and growth
378 phase. *J. Bacteriol.* 176, 5414–5422 (1994).
- 379 5. Asadulghani, M. et al. The defective prophage pool of *Escherichia coli* O157: prophage-
380 prophage interactions potentiate horizontal transfer of virulence determinants. *PLoS*
381 *Pathog.* 5, e1000408 (2009).
- 382 6. Wang, X. et al. Cryptic prophages help bacteria cope with adverse environments. *Nat.*
383 *Commun.* 1, 147 (2010).
- 384 7. Kobayashi, I., Nobusato, A., Kobayashi-Takahashi, N. & Uchiyama, I. Shaping the
385 genome--restriction-modification systems as mobile genetic elements. *Curr. Opin. Genet.*
386 *Dev.* 9, 649–656 (1999).
- 387 8. Van Melderer, L. & Saavedra De Bast, M. Bacterial Toxin–Antitoxin Systems: More
388 Than Selfish Entities? *PLoS Genet.* 5, e1000437 (2009).
- 389 9. Gerdes, K., Rasmussen, P. B. & Molin, S. Unique type of plasmid maintenance function:
390 postsegregational killing of plasmid-free cells. *Proc. Natl. Acad. Sci. U. S. A.* 83, 3116–
391 3120 (1986).

- 392 10. Allocati, N., Masulli, M., Di Ilio, C. & De Laurenzi, V. Die for the community: an
393 overview of programmed cell death in bacteria. *Cell Death Dis.* 6, e1609 (2015).
- 394 11. Vasu, K. & Nagaraja, V. Diverse Functions of Restriction-Modification Systems in
395 Addition to Cellular Defense. *Microbiol. Mol. Biol. Rev.* 77, 53–72 (2013).
- 396 12. Baba, T. et al. Construction of *Escherichia coli* K-12 in-frame, single-gene knockout
397 mutants: the Keio collection. *Mol. Syst. Biol.* 2, 2006.0008 (2006).
- 398 13. Hong, S. H., Wang, X. & Wood, T. K. Controlling biofilm formation, prophage excision
399 and cell death by rewiring global regulator H-NS of *Escherichia coli*. *Microb. Biotechnol.* 3,
400 344–356 (2010).
- 401 14. Conter, A., Bouché, J. P. & Dassain, M. Identification of a new inhibitor of essential
402 division gene *ftsZ* as the *kil* gene of defective prophage *Rac*. *J. Bacteriol.* 178, 5100–5104
403 (1996).
- 404 15. Sevin, E. W. & Barloy-Hubler, F. RASTA-Bacteria: a web-based tool for identifying
405 toxin-antitoxin loci in prokaryotes. *Genome Biol.* 8, R155 (2007).
- 406 16. von Mering, C. STRING: known and predicted protein-protein associations, integrated
407 and transferred across organisms. *Nucleic Acids Res.* 33, D433–D437 (2004).
- 408 17. Guo, Y. et al. *RalR* (a DNase) and *RalA* (a small RNA) form a type I toxin-antitoxin
409 system in *Escherichia coli*. *Nucleic Acids Res.* 42, 6448–6462 (2014).
- 410 18. Li, G.-W., Burkhardt, D., Gross, C. & Weissman, J. S. Quantifying Absolute Protein
411 Synthesis Rates Reveals Principles Underlying Allocation of Cellular Resources. *Cell* 157,
412 624–635 (2014).
- 413 19. Mahadevan, S., Reynolds, A. E. & Wright, A. Positive and negative regulation of the
414 *bgl* operon in *Escherichia coli*. *J. Bacteriol.* 169, 2570–2578 (1987).

- 415 20. Marianovsky, I., Aizenman, E., Engelberg-Kulka, H. & Glaser, G. The Regulation of the
416 *Escherichia coli* mazEF Promoter Involves an Unusual Alternating Palindrome. *J. Biol.*
417 *Chem.* 276, 5975–5984 (2001).
- 418 21. Brown, B. L., Lord, D. M., Grigoriu, S., Peti, W. & Page, R. The *Escherichia coli* toxin
419 MqsR destabilizes the transcriptional repression complex formed between the antitoxin
420 MqsA and the mqsRA operon promoter. *J. Biol. Chem.* 288, 1286–1294 (2013).
- 421 22. Ptashne, M. Principles of a switch. *Nat. Chem. Biol.* 7, 484–487 (2011).
- 422 23. García, P., Ladero, V., Alonso, J. C. & Suárez, J. E. Cooperative interaction of CI
423 protein regulates lysogeny of *Lactobacillus casei* by bacteriophage A2. *J. Virol.* 73, 3920–
424 3929 (1999).
- 425 24. Datsenko, K. A. & Wanner, B. L. One-step inactivation of chromosomal genes in
426 *Escherichia coli* K-12 using PCR products. *Proc. Natl. Acad. Sci. U. S. A.* 97, 6640–6645
427 (2000).
- 428 25. Uzzau, S., Figueroa-Bossi, N., Rubino, S. & Bossi, L. Epitope tagging of chromosomal
429 genes in *Salmonella*. *Proc. Natl. Acad. Sci. U. S. A.* 98, 15264–15269 (2001).
- 430 26. Kahramanoglou, C. et al. Direct and indirect effects of H-NS and Fis on global gene
431 expression control in *Escherichia coli*. *Nucleic Acids Res.* 39, 2073–2091 (2011).
- 432 27. Mukhopadhyay, A., Deplancke, B., Walhout, A. J. M. & Tissenbaum, H. A. Chromatin
433 immunoprecipitation (ChIP) coupled to detection by quantitative real-time PCR to study
434 transcription factor binding to DNA in *Caenorhabditis elegans*. *Nat. Protoc.* 3, 698–709
435 (2008).
- 436 28. Zaslaver, A. et al. Invariant Distribution of Promoter Activities in *Escherichia coli*. *PLoS*
437 *Comput. Biol.* 5, e1000545 (2009).

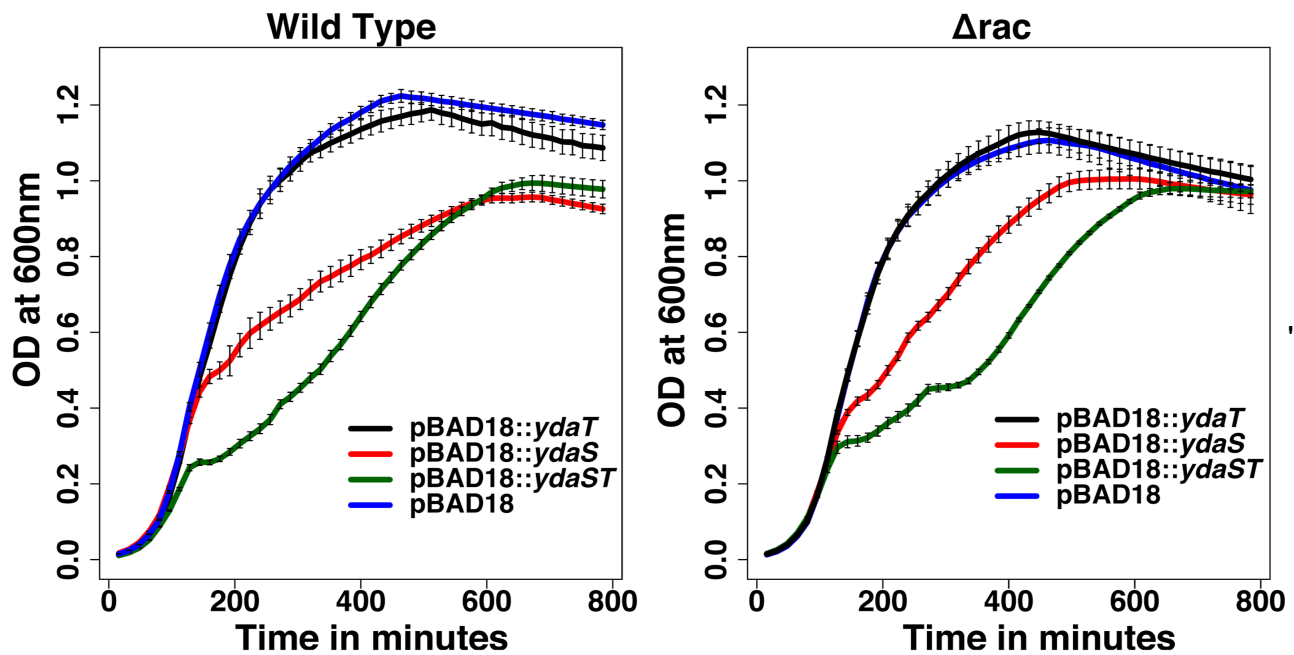
***Repression of YdaS Toxin is Mediated by Transcriptional Repressor
RacR in the cryptic rac prophage of Escherichia coli-K12***

Revathy Krishnamurthi^{1,2}, Swagatha Ghosh², Supriya Khedkar^{1,2} and Aswin Sai Narain Seshasayee²

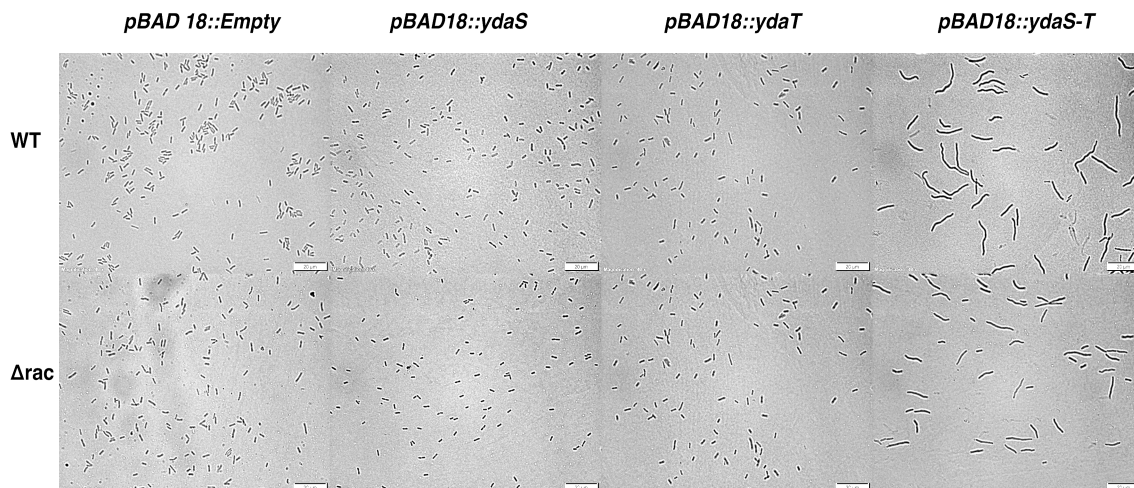
1. Shanmuga Arts, Science, Technology & Research Academy, Thanjavur, Tamil Nadu, India

2. National Centre for Biological Sciences, TIFR, Bangalore, India

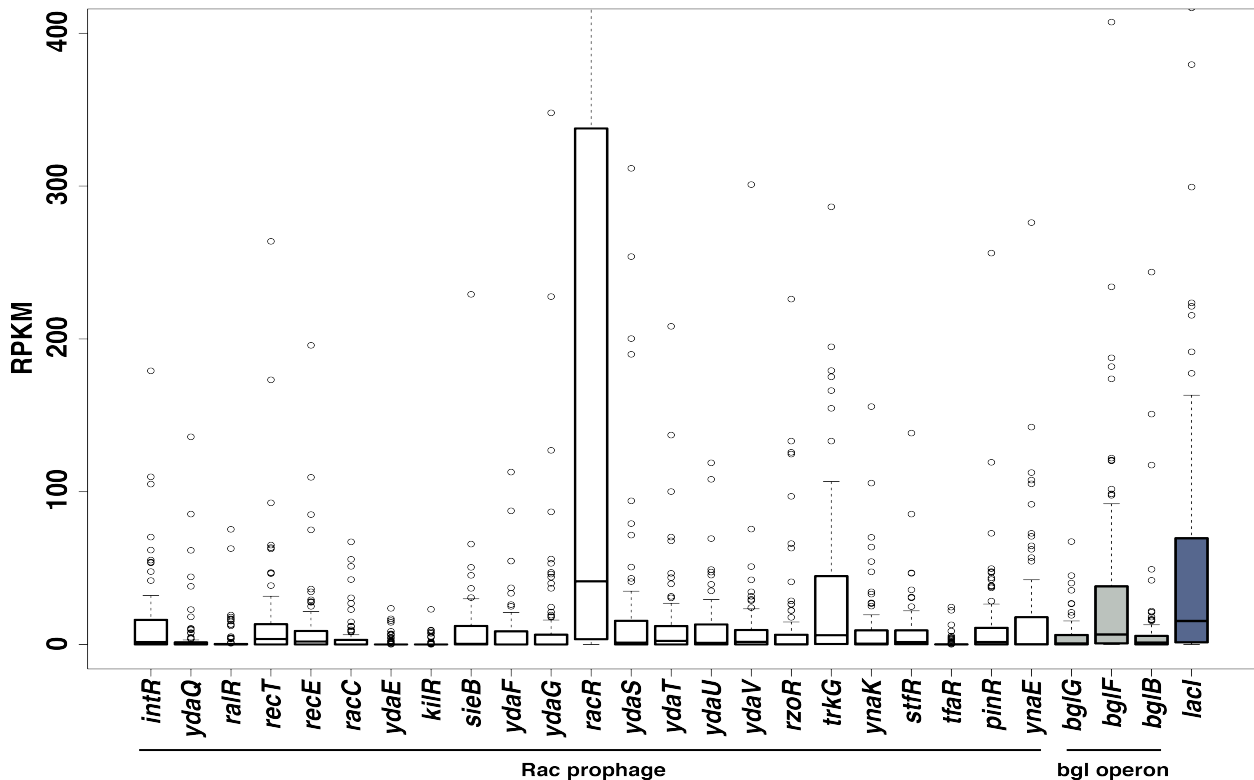
SUPPLEMENTARY INFORMATION



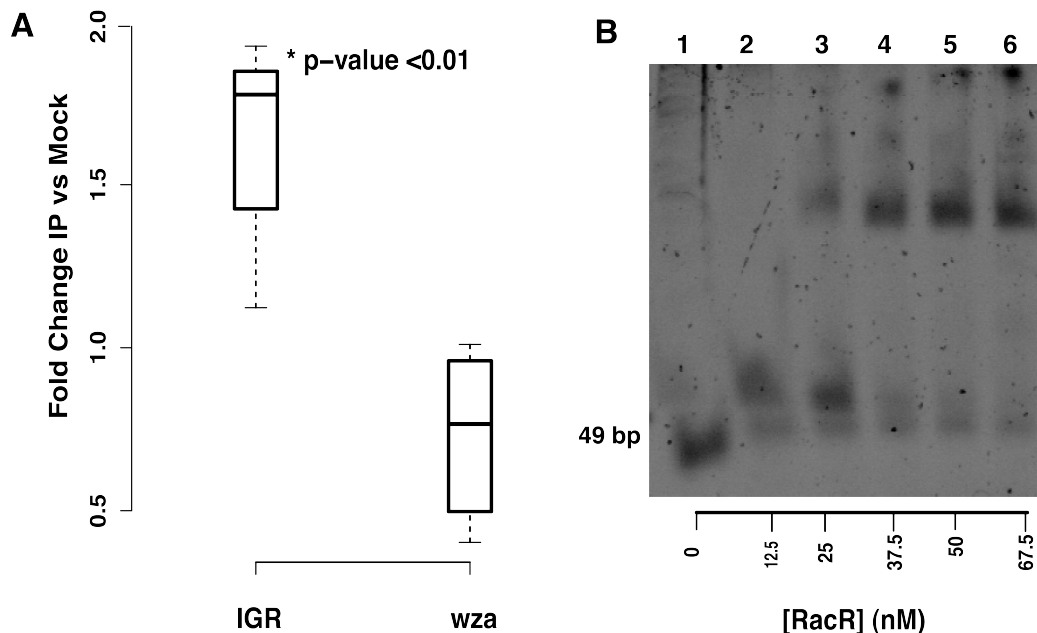
Supplementary Figure S1: Growth curve of the clones pBAD18-ydaS, pBAD18-ydaT, pBAD18-ydaS-T and Empty vector in wild type and in Δrac background showing that induction of ydaS and ydaS-T in tandem reduces the growth rate irrespective of the strains used



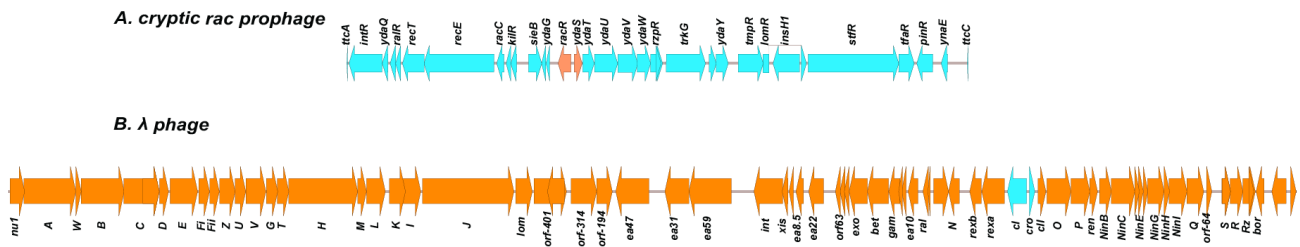
Supplementary Figure S2: Bright field images showing the increased cell size for the cells expressing ydaS-T when compared to the cells expressing ydaS or ydaT alone. Scale bar represents 20 μ m.



Supplementary Figure S3: Gene expression distribution of all the *rac* prophage genes is plotted as Reads Per Kilobase of transcripts per Million mapped reads (RPKM) from various RNA-Seq data. *RacR* is one of the few genes in the *rac* prophage found to be expressed across the conditions. *YdaS* and other toxins in the prophage is kept silent in par with the *bgl* operon genes.



Supplementary Figure S4: A) Chip q-PCR showing the enrichment for IGR in the Immuno Precipitated (IP'ed) DNA. Fold change was calculated by using $2^{-(\Delta\Delta Ct)}$ after normalizing the IP'ed and mock Ct to the Input Ct. Results are shown for the q-PCR done in triplicates for two biological replicate of IP'ed sample. * corresponds to $p < 0.01$; Wilcoxon rank sum test. B) EMSA showing the binding of *RacR* with 49bp region upstream *ydaS*. 23.5nM of 49 bp DNA was titrated against increasing concentration of *RacR* till 67.5 nM(Lane 2-6). Lane 1 shows 49bp without *RacR*.



Supplementary Figure S5: Comparison of rac prophage with lambda prophage. Rac prophage has lost most of its structural genes when compared to the lambda prophage. The regulatory genes in both the prophages are shown in different colors. Easyfig was used to generate the map of both prophages.

Supplementary Table1: Strains and plasmids used in this study

Strain Name	Description	Source
MG1655	F ⁻ , λ ⁻ , <i>rph-1</i>	CGSC
Δ <i>ydaF</i> -Δ <i>ydaT</i>	MG1655 Δ1419156-1421106 (<i>ydaF</i> - <i>ydaT</i>)	This study
Δ <i>sieB</i> -Δ <i>ydaU</i>	MG1655 Δ1418671-1421976 (<i>sieB</i> - <i>ydaU</i>)	This study
Δ <i>kilR</i> -Δ <i>ydaV</i>	MG1655 Δ1418008-1422729 (<i>kilR</i> - <i>ydaV</i>)	This study
Δ <i>recT</i> -Δ <i>trkG</i>	MG1655 Δ1413984-1425239 (<i>recT</i> - <i>trkG</i>)	This study
Δ <i>ralR</i> -Δ <i>ynaK</i>	MG1655 Δ1413733-1425640 (<i>ralR</i> - <i>ynaK</i>)	This study
Δ <i>ydaQ</i> -Δ <i>ynaA</i>	MG1655 Δ1413237-1427386 (<i>ydaQ</i> - <i>ynaA</i>)	This study
Δ <i>intR</i> -Δ <i>ttcC</i>	MG1655 Δ1411925-1434984 (<i>intR</i> - <i>ttcC</i> entire <i>rac</i> prophage)	This study
Δ <i>racR</i> -Δ <i>ydaS</i>	MG1655 Δ1420241-1420661 (<i>racR</i> - <i>ydaS</i> including the 123bp common IGR)	This study
Δ <i>ydaS</i> - <i>T</i>	MG1655 Δ1420365-1421106 (<i>ydaS</i> - <i>ydaT</i>)	This study
Δ <i>racR</i> Δ <i>ydaS</i> - <i>T</i>	MG1655 Δ <i>ydaS</i> , Δ <i>ydaT</i> , Δ <i>racR</i>	This study
Δ <i>kilR</i>	MG1655 Δ <i>kilR</i>	This study
Δ <i>ydaS</i>	MG1655 Δ <i>ydaS</i>	This study
Δ <i>ydaT</i>	MG1655 Δ <i>ydaT</i>	This study
Δ <i>ydaF</i>	MG1655 Δ <i>ydaF</i>	This study
Δ <i>ydaG</i>	MG1655 Δ <i>ydaG</i>	This study
<i>racR</i> ::3XFLAG	MG1655 <i>racR</i> ::3XFLAG	This study
<i>ydaS</i> ::3XFLAG	MG1655 <i>ydaS</i> ::3XFLAG	This study
C41(DE3)	OverExpress: F – ompT hsdSB (rB- mB-) gal dcm (DE3)	Lucigen
Plasmid	Description	Source
pBAD18	Arabinose Inducible vector	Gillian's lab
pBAD18:: <i>racR</i>	pBAD18 carrying <i>racR</i>	This study
pBAD18:: <i>ydaF</i>	pBAD18 carrying <i>ydaF</i>	This study
pBAD18:: <i>ydaG</i>	pBAD18 carrying <i>ydaG</i>	This study
pBAD18:: <i>ydaS</i>	pBAD18 carrying <i>ydaS</i>	This study
pBAD18:: <i>ydaT</i>	pBAD18 carrying <i>ydaT</i>	This study
pBAD18:: <i>ydaST</i>	pBAD18 carrying <i>ydaS</i> and <i>ydaT</i> in tandem	This study
pET28a	Overexpression Vector with C-Terminal His Tag	Novogen
pET28a:: <i>racR</i>	pET28a vector carrying <i>racR</i> gene with C-Terminal His Tag	This Study
pUA66	Low copy plasmid with fast folding GFP mut2	SAFS lab
pUA66::IGR	pUA66 vector carrying 123 bp <i>ydaS</i> promoter	This study
pKD13	F ⁻ , Δ(<i>araD</i> - <i>araB</i>)567, Δ <i>lacZ</i> 4787(::rrnB-3), Δ(<i>phoB</i> - <i>phoR</i>)580, λ ⁻ , <i>galU</i> 95, Δ <i>uidA</i> 3:: <i>pir</i> ⁺ , <i>recA</i> 1, <i>endA</i> 9(del-ins)::FRT, <i>rph-1</i> , Δ(<i>rhaD</i> - <i>rhaB</i>)568, <i>hsdR</i> 514, pKD13	CGSC
pKD3	F ⁻ , Δ(<i>araD</i> - <i>araB</i>)567, Δ <i>lacZ</i> 4787(::rrnB-3), Δ(<i>phoB</i> - <i>phoR</i>)580, λ ⁻ , <i>galU</i> 95, Δ <i>uidA</i> 3:: <i>pir</i> ⁺ , <i>recA</i> 1, <i>endA</i> 9(del-ins)::FRT, <i>rph-1</i> , Δ(<i>rhaD</i> - <i>rhaB</i>)568, <i>hsdR</i> 514, pKD3	CGSC
pKD46	F ⁻ , Δ(<i>araD</i> - <i>araB</i>)567, Δ <i>lacZ</i> 4787(::rrnB-3), λ ⁻ , <i>rph-1</i> , Δ(<i>rhaD</i> - <i>rhaB</i>)568, <i>hsdR</i> 514, pKD46	CGSC

pCP20	F ⁻ , $\Delta(\text{argF-lac})169$, $\phi 80\text{dlacZ58(M15)}$, <i>glnX44(AS)</i> , λ^- , <i>rfbC1</i> , <i>gyrA96(NalR)</i> , <i>recA1</i> , <i>endA1</i> , <i>spoT1</i> , <i>thiE1</i> , <i>hsdR17</i> , pCP20	CGSC
pSUB11	F ⁻ , $\Delta(\text{araD-araB})567$, $\Delta\text{lacZ4787}>::\text{rrnB-3}$, $\Delta(\text{phoB-phoR})580$, λ^- , <i>galU95</i> , $\Delta\text{uidA3}>::\text{pir}^+$, <i>recA1</i> , <i>endA9(del-ins)::FRT</i> , <i>rph-1</i> , $\Delta(\text{rhaD-rhaB})568$, <i>hsdR514</i> , pSUB11.	Gillian's lab.

Supplementary Table2: Primers used in this study

Primer Description	Sequence 5' -----> 3'
kilR_pkd13_F	ACCGCATCAACAAAGTTCATTTGTAAAAATGGAGATAATTgtgtaggctggagctgcttcg
kilR_pkd13_R	TTTTTGCAAAGGTGGTAAGCACATTTTATTTTCTTAGTCAattccggggatccgtcgacc
racR_pkd13_F	GGGATTGCCTAATGTAATGCGCATAGGAGAATATTAAGCAgtgtaggctggagctgcttcg
racR_pkd13_R	AATAACGGAATCCAGGAGTTTTCCGTCAGACCATATAAGTattccggggatccgtcgacc
ydaS_pkd13_F	GCGTCGCCTAATATTTCTGTGTGTTTTTGGAGTTCATTCCGAggttaggctggagctgcttcg
ydaS_pkd13_R	CTCATGCTTGATTTTCATGAATCATTTGCCTCTTGATGTTattccggggatccgtcgacc
ydaT_pkd13_F	CATTTGATCATACTGAAACATCAAGAGGCAAATGATTCAgtgtaggctggagctgcttcg
ydaT_pkd13_R	GTGGCTTAGAATAAGCACAAACAGCATGGAAACTTTTGCattccggggatccgtcgacc
intR ttcC F	ATTTTCAGTTCTCTGGTACTAAATGGGGCAAATTGGGGGCAAACTTTGCAAggttaggctggagctgcttcg
intR ttcC R	GCATGACGCATACTCTTCTGATGCCATATAACGAATTGAGTCGCTTTTAAattccggggatccgtcgacc
kilR ydaV F	TTCAACGTCTTTTTTGC AAAGGTGGTAAGCACATTTTATTCTTAGTCAgtgtaggctggagctgcttcg
kilR ydaV R	CTTTCAGTGCCTCAAAAACAGTCTCCATTAAATTTTTCTCCGGTAAAAAattccggggatccgtcgacc
ralR ynaK F	TTGTCCAGTTAGTAGGAGTGCCACCTTCCTTTTCAATAGTGCGGTAATTgtgtaggctggagctgcttcg
ralR ynaK R	TTTTCTCAATGTGGCGACGGATTAATGCATTACGGGAGCGATACTGATCGattccggggatccgtcgacc
recT trkG F	TCTCATAAAAAATATTTCAAGTTGGCGGTGCATTACACCGCCAGGCTGAAgtgtaggctggagctgcttcg
recT trkG R	ATGAGTGAGTCAACATAATATTAACCTCACAATTATAAATCAGCCATATAattccggggatccgtcgacc
sieB ydaU F	CGAGAGCTTGTGTTAACATTTCAATACCCTTACAGTTGAGAGTTATTGATgtgtaggctggagctgcttcg
sieB ydaU R	CTGCGGATACGTTCAAGAACATCGCCTGTCGCAATATTTTCATGGTCAGattccggggatccgtcgacc
ydaF ydaT F	TCCCATTTTATGAAGTTATTCTGGAACAGCAGGAGTAGACGTTTTAATCGgtgtaggctggagctgcttcg
ydaF ydaT R	GATGCTGCCCGGTGGCTTAGAATAAGCACAAACAGCATGGAAACTTTTGCattccggggatccgtcgacc
ydaQ ynaA F	TGCGAATGTATCTACCTCTAATCTCGACACCTGTTGGTAA

	TTTAGACATAggttaggctggagctgcttcg
ydaQ ynaA R	CATCGCATAACGCGCTGAACCATTTCATTACGCGCACAGACGGCCCCACCAattccggggatccgctgacc
racR_ydaS_IGR_F	CTCATGCTTGATTTTCATGAATCATTTCCTCTTGATGTTgttaggctggagctgcttcg
racR_ydaS_IGR_R	AATAACGGAATCCAGGAGTTTTCCGTCAGACCATATAAGTattccggggatccgctgacc
Tag RacR 3X F	AAGCTCTTGAATCTGAACGGAAAAGCCAGAACATCACAAAACTGGAAGTgactacaaagaccatgacgg
Tag RacR 3X R	GGGGGGGTTAAATAACGGAATCCAGGAGTTTTCCGTGACCATATAAGTcatatgaatatcctccttag
Tag ydaS 3X F	TGTCAGTGAAGCAACTAAATGACAGTAACAAATCCTCATTGATCATACCgactacaaagaccatgacgg
Tag ydaS 3X R	ATTCGATGTGCTCATGCTTGATTTTCATGAATCATTTCCTCTTGATGTTcatatgaatatcctccttag
ydaT _F_EcoRI	CCGGAATTC ATGAAAATCAAGCATGAGCACATCG
ydaT_R_Sall	CGGCGGGTCGACTTAATGAACAATGACAGAATCGTC
ydaS _F_EcoRI	CCGGAATTCATGAAAAAGAGAACTATTCATTCAAGC
ydaS _R_Sall	CGGCGGGTCGACTCAGGTATGATCAAATGAGGATTTG
racR_F_NdeI	CGCCATATGCTTAGTGGTAAAGAC
racR_R_XhoI	CCGCTCGAGAGTTCCAGTTTTTGTGAT
TSA_189_FW	CCGCTCGAGGATTTGACGGATCCCGATG
TSA_189_RV	AAAACCTGCAGTCAGGTATGATCAAATGAGG
TSA_whole_FW	CCGCTCGAGTTAAGTTCCAGTTTTTGTG
TSA-whole_RV	AAAACCTGCAGTCAGGTATGATCAAATGAGG
IGR_RT_FW	CGAATGAACTCCAAAAACACACAGA
IGR_RT_RV	TCCTATGCGCATTACATTAGGCA
wza_RT_FW	ATGATGAAATCCAAAATGAAATTGATGCC
wza_RT_RV	CATTTTGTGCGAGATCGAAATCAGCGTC
EMSA_123bp_F	CGAATGAACTCCAAAAACACACAGA
EMSA_123bp_R	TGCTTAATATTCTCCTA
EMSA_49bp_F	CGAATGAACTCCAAAAACACACAGA
EMSA_49bp_R	TTGCGTTAGGCGTCGCCTAATA
ydaS_Prom_XhoI_F	CCGCTCGAGTGCTTAATATTCTCCTATGC
ydaS_Prom_R_BamHI	CGCGGATCCCGAATGAACTCCAAAAACA

Supplementary Table 3: List of accession numbers of RNA seq data used for calculating RPKM

GSE63858	Ribosome profiling of <i>E. coli</i> K-12 MG1655 MOPS rich media with 0.2% glucose
GSE72899	Clarifying the translational pausing landscape in bacteria by ribosome profiling [1]
GSE72899	COLOMBOS v2.0: an ever expanding collection of bacterial expression compendia [2]
E-MTAB-2802	Comprehensive Mapping of the <i>Escherichia coli</i> Flagellar Regulatory Network [3]
GSE54901	Deciphering Fur transcriptional regulatory network highlights its complex role [4]
GSE66482	Decoding genome-wide GadEWX-transcriptional regulatory networks reveals multifaceted cellular responses to acid stress in <i>Escherichia coli</i> [5]
GSE46740	Genome-scale reconstruction of the sigma factor network in <i>Escherichia coli</i> : topology and functional states [6]
E-MTAB-2903	Identification of bacterial sRNA regulatory targets using ribosome profiling [7]
GSE55199	Global Transcriptional Start Site Mapping Using Differential RNA Sequencing Reveals Novel Antisense RNAs in <i>Escherichia coli</i> [8]
GSE41940	Rho and NusG suppress pervasive antisense transcription in <i>Escherichia coli</i> [9]
E-MTAB-4240	SuhB Associates with Nus Factors To Facilitate 30S Ribosome Biogenesis in <i>Escherichia coli</i> [10]

GSE69856	The ribonuclease polynucleotide phosphorylase can interact with small regulatory RNAs in both protective and degradative modes [11]
GSE82343	Modulation of global transcriptional regulatory networks as a strategy for increasing kanamycin resistance of EF-G mutants
GSE40313	Genomic analysis reveals epistatic silencing of "expensive" genes in Escherichia coli K-12 [12]
In house RNA seq Data	Transcriptome data for wild type , Δfis , Δcya mutants in Early Exponential, Mid Exponential growth phase

BIBLIOGRAPHY

1. Mohammad, F., Woolstenhulme, C. J., Green, R. & Buskirk, A. R. Clarifying the Translational Pausing Landscape in Bacteria by Ribosome Profiling. *Cell Rep.* **14**, 686–694 (2016).
2. Meysman, P. *et al.* COLOMBOS v2.0: an ever expanding collection of bacterial expression compendia: Table 1. *Nucleic Acids Res.* **42**, D649–D653 (2014).
3. Fitzgerald, D. M., Bonocora, R. P. & Wade, J. T. Comprehensive Mapping of the *Escherichia coli* Flagellar Regulatory Network. *PLoS Genet.* **10**, e1004649 (2014).
4. Seo, S. W. *et al.* Deciphering Fur transcriptional regulatory network highlights its complex role beyond iron metabolism in *Escherichia coli*. *Nat. Commun.* **5**, 4910 (2014).
5. Seo, S. W., Kim, D., O'Brien, E. J., Szubin, R. & Palsson, B. O. Decoding genome-wide GadEWX-transcriptional regulatory networks reveals multifaceted cellular responses to acid stress in *Escherichia coli*. *Nat. Commun.* **6**, 7970 (2015).
6. Cho, B.-K., Kim, D., Knight, E. M., Zengler, K. & Palsson, B. O. Genome-scale reconstruction of the sigma factor network in *Escherichia coli*: topology and functional states. *BMC Biol.* **12**, 4 (2014).
7. Wang, J. *et al.* Identification of bacterial sRNA regulatory targets using ribosome profiling. *Nucleic Acids Res.* gkv1158 (2015). doi:10.1093/nar/gkv1158
8. Thomason, M. K. *et al.* Global Transcriptional Start Site Mapping Using Differential RNA Sequencing Reveals Novel Antisense RNAs in *Escherichia coli*. *J. Bacteriol.* **197**, 18–28 (2015).
9. Peters, J. M. *et al.* Rho and NusG suppress pervasive antisense transcription in *Escherichia coli*. *Genes Dev.* **26**, 2621–2633 (2012).
10. Singh, N. *et al.* SuhB Associates with Nus Factors To Facilitate 30S Ribosome Biogenesis in *Escherichia coli*. *mBio* **7**, e00114-16 (2016).
11. Bandyra, K. J., Sinha, D., Syrjanen, J., Luisi, B. F. & De Lay, N. R. The ribonuclease polynucleotide phosphorylase can interact with small regulatory RNAs in both protective and degradative modes. *RNA* **22**, 360–372 (2016).
12. Srinivasan, R. *et al.* Genomic analysis reveals epistatic silencing of 'expensive' genes in *Escherichia coli* K-12. *Mol. Biosyst.* **9**, 2021 (2013).